PREDICTIONS OF IMPINGING FLOWS WITH
LOW-REYNOLDS NUMBER TURBULENCE MODELS

Abstract

Several low-Reynolds number k-ε turbulence models have been used to simulate the flow and heat transfer in slot confined and circular unconfined impinging jet configurations. Predictions for the velocity with its fluctuation and Nusselt number are compared to available experimental data. The relative performance of the models is assessed. It has been found that results obtained for the velocity parallel to the plate are in agreement with experimental data but none of models are entirely successful in predicting the radial Reynolds normal stress. For heat transfer, an additional source term in the equation of ε was necessary for reducing near-wall length scales and improving the near-transfer predictions by means of the low-Reynolds number k-ε turbulence models.

Keywords: *impinging jet, turbulence, numerical simulation, low-Reynolds number.*

Résumé

Une série de modèles de turbulence k-ε à bas nombre de Reynolds est utilisée pour simuler numériquement l'écoulement d'un jet à point de stagnation dans deux configurations (isotherme confiné et libre avec un transfert thermique à la paroi). Les résultats de calcul de la vitesse parallèle à la paroi, de sa fluctuation et du nombre de Nusselt sont confrontés aux mesures existant dans la littérature. On trouve une bonne concordance pour la composante de la vitesse, par contre aucun des modèles n'est capable de prédire exactement la composante du tenseur de Reynolds turbulent correspondante. L'ajout d'un terme dans l'équation de transport de ε s'avère indispensable pour réduire l'échelle de longueur prés de la paroi et par conséquent améliorer la prédiction du transfert de chaleur gaz-paroi par ce type de modèles.

Mots clés: *jet heurtant, turbulence, simulation numérique, bas-nombre de Reynolds.*

Redjem HADEF
Amar HADEF
Institute of mechanical Engineering
University Larbi Ben M'hidi
BP 297, Oum El Bouaghi (Algeria)

ملخص

نستعمل مجموعة من نماذج الاضطراب k-ε ذا عدد رينولدس صغير لحساب رقمي لسيلان دفع غازي لنقطة توقف في شكلين (محبوس مع حرارة ثابتة، حر بتحويل حراري للجدار). وقورنت من قبل نتائج حسابات السرعة الموازية للجدار، تقلباتها وعدد نوسلت بالمقاييس الموجودة. نجد توافق جيد لإحداثية السرعة، لكن تعجز كل النماذج عن تكهن دقيق لإحداثية موتر رينولدس المضطرب الموافق. زيادة حد في معادلة ε ضروري لخفض سلم الطول بجانب الجدار وينتج عن ذلك تحسين التنبؤ الحسابي لتحويل الحرارة بين الغاز والحائط بهذا النوع من النموذج.

الكلمات المفتاحية: دفع مصطدم، الاضطراب، تنبؤ رقمي، عدد صغير لرينولدس.

The k-ε model is one of the most popular turbulence models and is nowadays used in many practical flow simulations. The great majority of these computations is carried out with the application of the so-called wall functions that relate surface boundary conditions to points in the fluid away from the boundaries and thereby avoid the problem of modelling the direct influence of viscosity with the aid of empirical relations. The latter are based on the assumptions of universal logarithmic velocity and temperature profiles, a local equilibrium of turbulence and a constant near-wall shear stress layer. However, for most of the applications of industrial interest, such as turbulent boundary layers at low Reynolds numbers, separated flows and the flow over surfaces with heat and/or mass transfer, these assumptions lose their validity, eventually leading to inaccurate results. Because of these shortcomings, many modifications have been made over the past two decades to extend the k-ε model for use at low Reynolds numbers and to describe accurately the flow behaviours close to a solid wall. These models are generally derived from high-Reynolds models by incorporating either a wall damping effect, a direct effect of molecular viscosity, or both, on the empirical constants and functions in the turbulence-transport equations [1,2]. Most of them have been developed using fully developed pipe flow conditions [3,4]. Although this case tends to be well reproduced, reports of impinging jet simulations are scarce and often incomplete [5]. Due to the complexity of the flow field which includes entrainment, stagnation, change of flow direction and streamline curvature, the impinging jet is a challenging test case for validation of turbulence models.

In the present contribution, five low-Reynolds-number k-ε turbulence models are judged by assessment of their performance in predicting

impinging flows as far as experimental data are available. The configurations considered for the evaluation are a two dimensional isothermal semi-confined slot jet flow and an axisymmetric free jet with heat transfer. The comparisons are limited to the mean radial velocity and its fluctuation profiles in the near-wall region for the first case and to the local heat transfer distribution for the second one.

MATHEMATICAL MODEL AND ANALYSIS

Conservation equations

The basic set equations used to describe incompressible turbulent flow are the continuity, momentum and energy equations. Applying the so-called steady state Reynolds averaging, we have:

$$\vec{\nabla}.\vec{U} = 0 \tag{1}$$

$$\vec{\nabla}.\vec{U}\vec{U} = -\vec{\nabla} P/\rho + \vec{\nabla}.\left[(\nu+\nu_t)\left(\vec{\nabla}\vec{U}+\vec{\nabla}\cdot\vec{U}\right)\right] \tag{2}$$

$$\vec{\nabla}.\vec{U}T = \vec{\nabla}.\left[\left(\frac{\nu}{Pr}+\frac{\nu_t}{Pr_t}\right)\vec{\nabla}T\right] \tag{3}$$

The turbulent Prandtl number Pr_t is given by the Kays and Crawford [6] correlation:

$$Pr_t = \frac{1}{0.588 + 0.288(\nu_t/\nu) - 0.0441(\nu_t/\nu)^2\left[1-\exp\left(-5.165/(\nu_t/\nu)\right)\right]} \tag{4}$$

This correlation has been derived in order to fit the variations of Pr_t from about 1.8 at the wall to 0.8 far from it, and provides reasonable values in most of the applications.

The k-ε model relates the turbulence viscosity, ν_t, to the turbulence kinetic energy, k, and the turbulence dissipation rate, ε, using:

$$\nu_t = f_\mu C_\mu \frac{k^2}{\varepsilon} \tag{5}$$

where C_μ is a constant of the turbulence model. The transport equations for k and ε are as follows:

$$\vec{\nabla}.\vec{U}k - \vec{\nabla}.\left[\left(\nu+\frac{\nu_t}{\sigma_k}\right)\vec{\nabla}k\right] = P_k - (\varepsilon+D) \tag{6}$$

$$\vec{\nabla}.\vec{U}\varepsilon - \vec{\nabla}.\left[\left(\nu+\frac{\nu_t}{\sigma_\varepsilon}\right)\vec{\nabla}\varepsilon\right] = (f_1 C_1 P - f_2 C_2 \varepsilon)\frac{\varepsilon}{k} + E \tag{7}$$

where $\sigma_k, \sigma_\varepsilon\ C_1$ and C_2 are also constants used in the turbulence models. P_k is the shear production defined by:

$$P_k = \nu_t \vec{\nabla}\vec{U}.\left[\vec{\nabla}\vec{U}+\left(\vec{\nabla}\vec{U}\right)\right] \tag{8}$$

The functions f_μ, f_1, f_2 and, in some cases, the extra terms D and E, are introduced to improve the turbulence modelling in regions close to solid walls where viscous effects dominate over turbulent ones. Different formulae have been suggested to calculate the terms above and due to a lack of reliable experimental data these near-wall modifications have been largely based on dimensional

reasoning, intuition and indirect testing by comparing model results for global flow parameters like skin friction coefficients, heat transfer rates, etc., with experiments. The turbulence models considered here are those of Jones and Launder (denoted by JL) [7], Launder and Sharma (LS) [8], Lam and Bremhorst (LB) [9], Chien (CH) [10], and Abe *et al*. (AK) [11]. Other low-Reynolds number models reported in the literature are not tested here as they fail to reproduce even the impinging jet [12]. For the empirical constants, a common value is taken for $C_\mu = 0.09$ but others with the wall boundary condition for ε depend slightly on the models as given in Table 1. The functions together with the additional terms are summarised in Table 2.

Boundary conditions

Along the centreline, the symmetry conditions were employed for all variables except the radial velocity component whose value was set to zero. On the wall the radial and normal velocity components were set to zero, the non-slip condition was imposed on the turbulence kinetic energy and the dissipation was as given in Table 1. At the outflow boundary the velocity normal to the boundary was obtained from the continuity and zero gradient values of the other variables were applied. The inlet conditions specified for each of the flows considered are discussed in the respective section.

Numerical resolution

The governing equations of the transport processes, controlled by diffusion and convection, can be cast into a general form as:

$$\nabla.\left[r^n\left(\rho\vec{U}\phi - \Gamma_\phi\nabla\phi\right)\right] = r^n S_\phi \tag{9}$$

where the geometry index n has a value of 0 for planar and 1 for the axisymmetric coordinate, $\phi = 1, U, V, k, \varepsilon, T$ is the general dependent variable, S_ϕ is the volumetric source of ϕ and Γ_ϕ is the diffusion coefficient for ϕ.

The equation set was discretised using the control volume method [13]. The convection terms in the momentum equations were approximated using a form of the three-point QUICK scheme [14]. The convection terms for the scalar variables were computed using Hybrid Differencing [15]. The PISO algorithm [16] with a standard TDMA solver was used to handle the pressure-coupling. At least 21 nodes were employed within the viscous sublayer region in these models, to predict the wall shear stress. The convergence criterion adopted in the present work is that the summation of the absolute mass residuals normalised by the inlet mass, in the entire computational domain is less than 1%.

RESULTS AND DISCUSSION

Confined isothermal impinging flow

The performance of the selected models is first in contrast to experimental data of a turbulent slot jet impinging normally on a target surface [17]. The impingement region is confined by means of a confinement

87

**Table 1:** Values of the constants and extra terms for the low-Re $k\text{-}\varepsilon$ models.

Models	ε_{wall}	C_1	C_2	σ_k	σ_ε	D	E
JL	0	1.45	1.9	1.0	1.3	$2\nu\left(\partial\sqrt{k}/\partial x\right)^2$	$2\nu\nu_t\left(\partial^2 V/\partial x^2\right)^2$
LS	0	1.45	1.9	1.0	1.3	$2\nu\left(\partial\sqrt{k}/\partial x\right)^2$	$2\nu\nu_t\left(\partial^2 V/\partial x^2\right)^2$
LB	$\left(\partial\varepsilon/\partial x\right)_w = 0$	1.44	1.92	1.0	1.3	0	0
CH	0	1.35	1.8	1.0	1.3	$2\nu\left(k/x^2\right)$	$-2\nu\left(\varepsilon/x^2\right)\exp-0.5x^+$
AK	$\nu\left(\partial^2\varepsilon/\partial x^2\right)_w = 0$	1.5	2.0	1.4	1.4	0	0

Table 2: Damping functions for the low-Re $k\text{-}\varepsilon$ models.

Models	f_μ	f_1	f_2
JL	$\exp\dfrac{-2.5}{1+\text{Re}_t/50}$	1	$1.-0.3\exp-\text{Re}_t^2$
LS	$\exp\dfrac{-3.4}{\left(1+\text{Re}_t/50\right)^2}$	1	$1.-0.3\exp-\text{Re}_t^2$
LB	$\dfrac{\left(1-\exp-0.0165\,\text{Re}_k\right)^2}{\left[1+20.5/\text{Re}_t\right]}$	$1+\left(0.05/f_\mu\right)^3$	$1.-\exp-\text{Re}_t^2$
CH	$1-\exp-0.015x^+$	1	$1.-0.22\exp-\text{Re}_t^2/36$
AK	$\left(1-\exp-\text{Re}_\varepsilon/14\right)^2$ $\left[1+\left(5/\text{Re}_t^{3/4}\right)\quad\exp-\left(\text{Re}_t/200\right)^2\right]$	1	$\left(1-\exp-\text{Re}_\varepsilon/3.1\right)^2$ $\left[1-0.3\exp-\left(\text{Re}_t/6.5\right)^2\right]$

plate that is flush with the slot and parallel to the impingement plate (Fig. 1). The slot jet width B was 40 mm and the distance of the impingement wall from the wall was four times the slot width. Both the confinement and the impingement plate extend in the y-direction to $y=\pm 13B$ and the Reynolds number based on the slot width and the bulk velocity, U_b, was 20000. The mean and root mean square axial velocity distributions across the width of the jet exit have been found (measured) to be uniform and equal to U_b and 0.009 U_b, respectively. Given the turbulence intensity, the inlet turbulence kinetic energy and dissipation rates are calculated from:

$$k = u'^2 \quad\text{and}\quad \varepsilon = C_\mu\frac{k^{3/2}}{0.03\quad(B/2)} \tag{10}$$
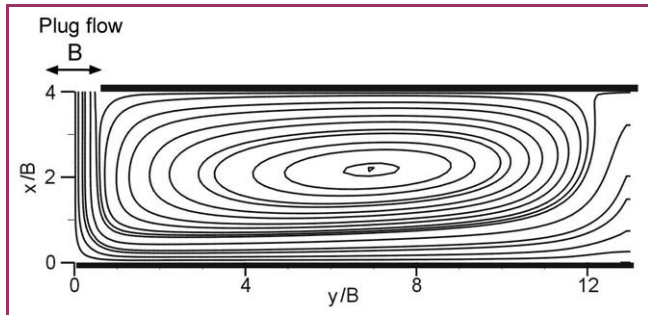
Figure 1: Configuration and streamlines for the confined slot-jet.

Grid densities of sizes 65x85 and 100x120 which were non uniform in both the x and y direction, were used to check the grid independence, and the 65x85 grid was found to be adequate. The first grid node near the wall was placed at $x^+ \approx 0.08$ to ensure the adequate resolution of the viscous sublayer.

Experimental measurements of mean and root mean square radial velocity were obtained by means of a hot-wire anemometer with an uncertainly of 11% in mean velocity, 6% in root mean square velocity normalized with respect to U_b, and 9% in distance. The axial profiles of mean radial velocity normalised with respect to the bulk velocity are shown in figure 2. These axial profiles are presented for radial distances corresponding to y/B = 2, 4, 7 and 9 as the flow develops from the stagnation point. It should first be noted that the results of JL and LS are identical and the maximum normalized mean velocity exceeds 0.96. The latter behaviour reflects the fact that the impingement wall is located within the potential core (95% criterion). All five models predictions closely follow the mean radial velocity measurements up to y = 7B, beyond which the data are over-predicted. This could be anticipated since the models were developed for this type of flow. However the best prediction of the mean radial velocity is produced by the JL and LS models, which accurately predict the value of the peak mean radial velocity.

Figure 3 compares the calculated and measured normalized turbulent velocity parallel to the wall at different
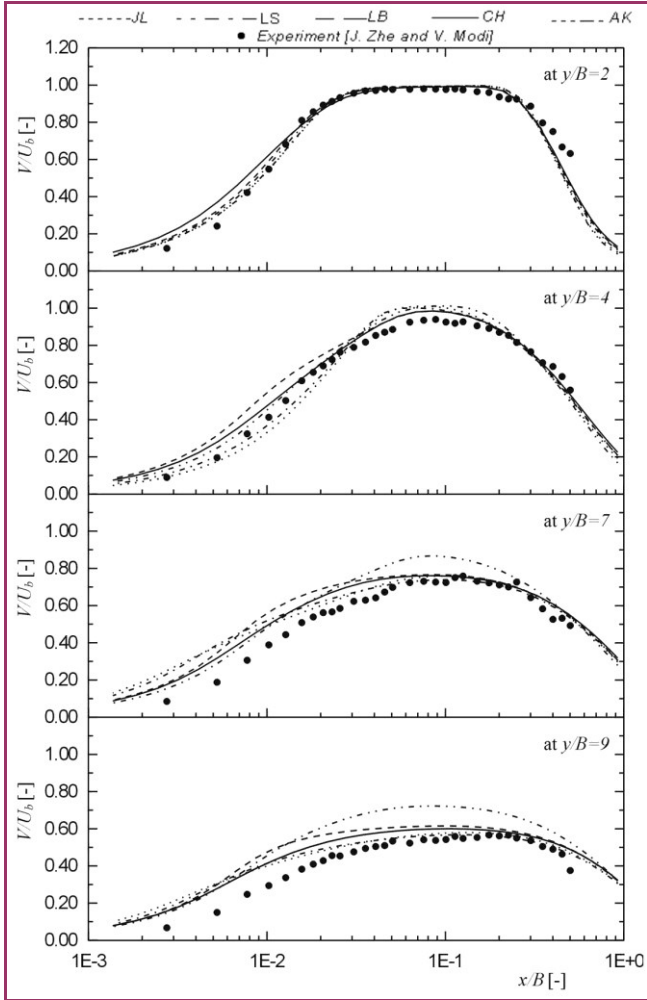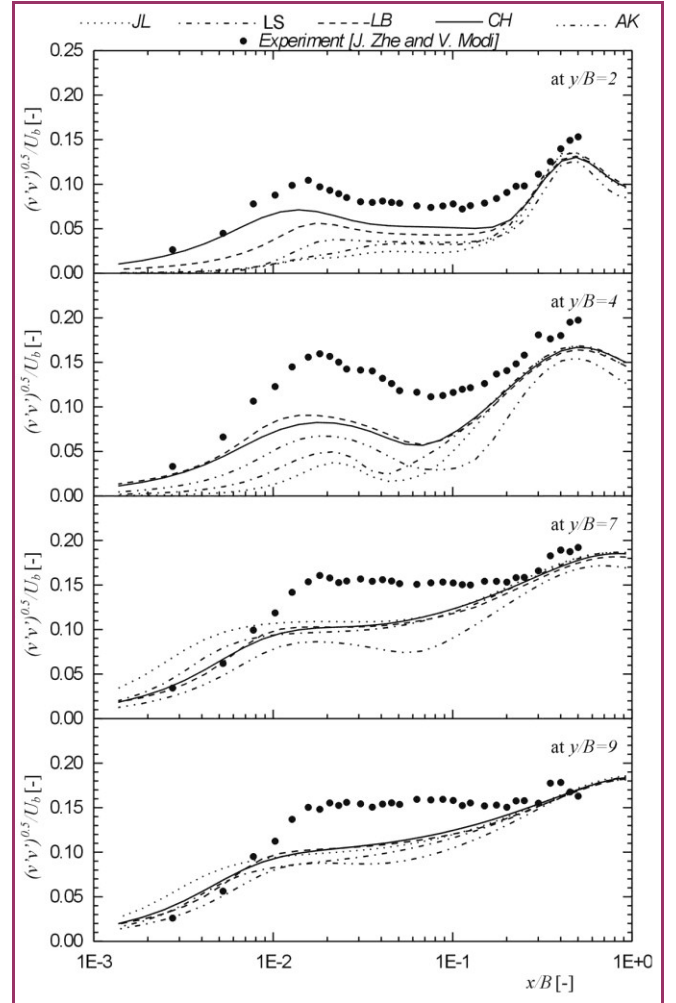
Figure 2: Variation of mean velocity V/U_b with x/B along impingement wall.

Figure 3: Variation of $(v'v')^{0.5}/U_b$ with x/B along impingement wall.

stations. It is apparent that none of the models fits the data well. However, the results of LB and CH show fair agreement with the location of the rms maximum and reproduce only the qualitative features. This poor prediction arises mainly from the use of the eddy-viscosity stress-strain law to represent parallel stresses:

$$\overline{v'^2} = -2\nu_t \frac{\partial \overline{V}}{\partial y} + \frac{2}{3}\overline{k} \tag{11}$$

This is initially a marked increase of v'/U_b as one moves away from the axis of symmetry both near the wall and further away. The increase near the wall arises from the shear induced by the flow's acceleration from the stagnation point. The increase at greater distances from the wall simply shows that the line of traverse passes through a more energetic part of the turbulent mixing layer originating from the slot lip. At greater distances from the stagnation point, streamlines are nearly parallel to the surface and, significantly, the fluctuating velocities grow for a time. As the shear weakens, however, levels fall gradually with increasing the distance from the jet-axis and the turbulent intensity takes on a virtually uniform level from the edge of the sublayer to the half width of the wall jet.

Unconfined circular jet with heat transfer

The performance of the selected models is further compared with the data of the fully developed axisymmetric flow [18]. The schematic picture of the flow is shown in figure 4 where the pipe was 26 mm internal diameter and 2.1 m in length, and the rectangular test plate on which the flow impinged measured 1275x975 mm. The impingement plate temperature was kept at 10K above that of the inlet fluid (300 K).. Experiments were carried out with a Reynolds number of 23750 and measurements extended up to $r/d = 9$. The mean axial velocity at the pipe inlet was specified by means of the $1/7^{th}$ power law for turbulent flow:

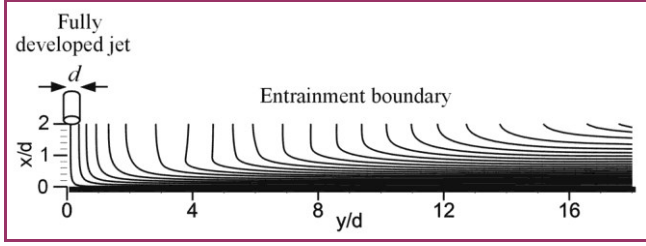$$U(r) = U_{cl} \left(1 - r/R\right)^{1/7} \tag{12}$$

The connection between centre-line and bulk velocities as a function of Reynolds number is given by [19]:

$$U_d / U_{cl} = 0.811 + 0.038 \left(\log_{10} \text{Re} - 4\right) \tag{13}$$

The inlet profiles of k and ε are given by:

$$k_e = \frac{0.91 \, U_\tau^2}{(r/R) + 0.14} \tag{14}$$

$$\varepsilon = C_\mu \frac{k^{3/2}}{0.03 \, (d/2)} \tag{15}$$

Figure 4: Configuration and streamlines for the impinging free round-jet.

The friction velocity along the nozzle, U_τ, is approximated by the following relation [20]

$$\frac{U_b}{U_\tau} = 2.5 \ln\left(\frac{U_\tau d}{2\nu}\right) + 1.5 \tag{16}$$

Over the remainder of the upper boundary, zero-gradients values are assigned to k *and* ε. The velocity normal to the boundary has been obtained from continuity and the temperature has been set to To. In the present geometry, a measured Nusselt number distribution is available for comparison. Because steep temperature variation occurs in the thin near-wall region, the near-wall turbulence structure strongly influences the wall heat transfer characteristics. Consequently, near-wall turbulence modelling plays an important role in reproducing the correct heat transfer characteristics. Figure 5 compares the calculated Nu distribution with data for an impingement at $H/d = 2$. The results predicted by the five models group themselves in pair: the models of JL and LS produce excessive levels of Nusselt number due, we suggest, to the far too high turbulence energy while the other ones do rather better, predicting at least qualitatively the decrease in Nusselt number with radius that occurs for $r/d > 2$. However, these last three models overpredict Nu in the stagnation region and the model of CH predicts the location of its maximum to occur away from the stagnation point at $r/d \approx 0.5$. One notes that all the models capture qualitatively the increase in Nu with radius that occurs in the range $1.2 < r/d < 2.0$. The peak is more pronounced at small H/d, decreasing in prominence and moving radially from the jet axis as H/d increases. This peak is attributed to the transition from laminar to a turbulent boundary layer in the spreading wall jet.

It is interesting to note in figure 6 the importance of the additional term in the ε equation referred to as the 'Yap correction' [21] and expressed as:

$$S_{\varepsilon,yap} = Max\left(C_{yap}\left(\frac{l}{l_e}-1\right)\left(\frac{l}{l_e}\right)^2 \frac{\varepsilon^2}{k}, 0\right) \tag{17}$$

The term has only minor effect on the turbulent velocity and none at all on the mean velocity. It also achieves its effect through limiting the departure of the near-wall length scale from its equilibrium level, thus raising levels of ε and reducing k. With its inclusion, the turbulence models predicted considerably lower Nusselt number values. In the stagnation region $(r/d \leq 1.5)$, the predicted values were reduced to levels comparable to measurements with the CH,
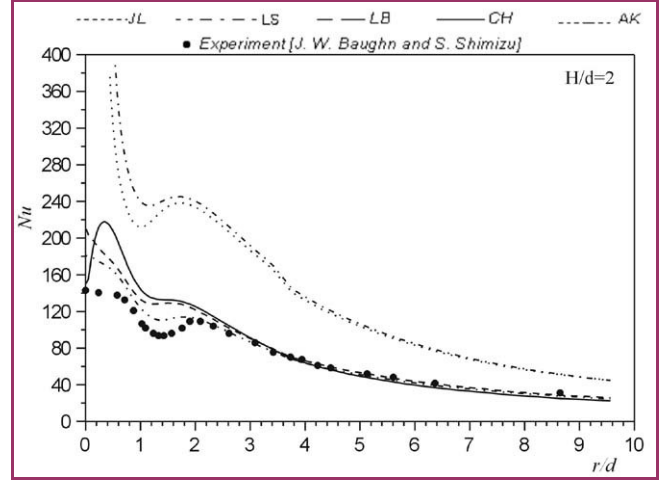
Figure 5: Nusselt number distribution without the Yap correction.
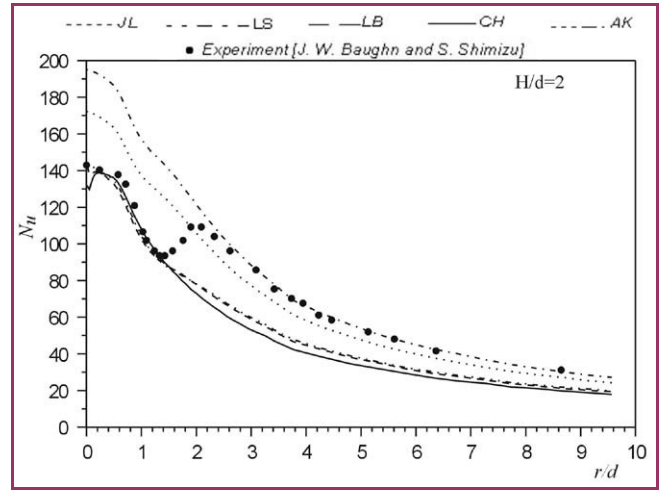
Figure 6: Nusselt number distribution with the Yap correction.

LB and AK models but overestimated with the others ones. Far downstream the CH model, like the LB and AK models, contrary to the JL and LS models predicted poorly the turbulent convection heat transfer. In addition, none of the models captures the existence of the secondary peak in the Nu-profile. The reason is that the secondary source was developed by Yap for improvement the prediction of the LS model to the abrupt-pipe expansion problem, and hence may not be exactly for this configuration. By preserving the general form of the $S_{\varepsilon,yap}$ and adjusting only the constant C_{yap}, it should be possible to improve the prediction accuracy.

CONCLUSION

A comparison has been presented of the performance of five low-Reynolds k-ε turbulence model in predicting the dynamic and thermal characteristics of the near-impingement region of the turbulent impinging jet.

In the confined slot-jet, all five models produced good predictions of the mean velocity profile. The closest agreement with experimental data was obtained with the CH model. However, all models predicted the velocity fluctuation poorly because of the weakness of the eddy viscosity stress-strain relation to represent the parallel stresses.

In the unconfined axisymmetric-jet, the convective heat-transfer calculations are extremely sensitive to the near wall model used. All five low-Reynolds number models predicted excessively large length scales near the wall, but upon addition of a secondary source term in the turbulence dissipation equation, fairly agreement with experimental data was obtained. This secondary source term was found to be inappropriate for heat-transfer predictions in stagnation flow, because it has been initially developed for the re-attachment flow. Based on the results of this study, the AK model is recommended for simulating heat-transfer in stagnation flow.

NOMENCLATURE

B : width of the slot

C_{yap} : constant for the Yap correction

C_1, C_2 : constants in the ε transport equation

C_μ : constant in v_t of k-ε model

d : nozzle inner diameter

f_1, f_2 : function modifying C_1 and C_2 in ε equation

f_μ : function modifying v_t in the k-ε model

D, E : turbulence model functions

H : jet-to-plate distance

k : turbulence kinetic energy

l : turbulent length scale $(=2.45x)$

l_e : equilibrium length scale $(=k^{1.5}/\varepsilon)$

Nu : local Nusselt number

P : pressure

P_k : rate of generation of kinetic energy

Pr : Prandtl number $(=0.7)$

Pr_t : turbulent Prandtl number

R : nozzle inner radius

r : radial coordinate

Re : flow Reynolds number

Re_k : turbulent Reynolds number $\left(=\sqrt{k}\,x/v\right)$

Re_t : turbulent Reynolds number $\left(=k^2/v\varepsilon\right)$

Re_ε : turbulent Reynolds number $\left(=(v\varepsilon)^{0.25}x/v\right)$

T : temperature

T : temperature of the incoming flow

$\vec{U}$: mean velocity vector

U : axial mean velocity

U_b : bulk velocity in the slot jet

U_{cl} : mean axial velocity at the centre-line of the jet

U_d : bulk velocity in the circular jet

U_τ : friction velocity along the nozzle

V : radial mean velocity

V_τ : friction velocity along the impinging wall

v' : radial mean velocity fluctuation

x : distance from the impinging wall

x^+ : normalized wall coordinate $(=xV_\tau/v)$

v : fluid kinematic viscosity

v_t : turbulent kinematic viscosity

ε : dissipation rate of turbulence energy

ρ : fluid density

σ_k : turbulent Prandtl number for diffusion of k

σ_ε : turbulent Prandtl number for diffusion of ε

REFERENCES

[1]- Craft T.J., Launder B.E. and Suga K., "Development and application of a cubic eddy-viscosity model of turbulence", *Int. J. Heat and Fluid Flow*, **17**, (1996), pp.108-115.

[2]- Jacovides H. and Raisee M., "Recent progress in the computation of flow and heat transfer in internal cooling passages of turbines blades", *Int. J. Heat and Fluid Flow*, **20**, (1999), pp.320-328.

[3]- Michelassi V., Rodi W. and Zhu J., "Testing a low Reynolds number k-ε turbulence model based on direct simulation data", Research report SFB 210/T/83 University of Karlsruhe, (1993).

[4]- Martinuzzi R. and Pollard A., "Comparative study of turbulence models in predicting turbulent pipe flow-Algebraic stress and k-ε models", *AIAA journal*, **27-1**, (1989), pp.29-36.

[5]- Craft T.J., Graham L.J.W. and Launder B.E., "Iminging jet studies for turbulence model assessment-II. An examination of the performance of four turbulence models", *Int. J. Heat Mass Transfer*, **36-10**, (1993), pp. 2685-2697.

[6]- Kays W.M. and Crawford M.E., Convective heat and mass Transfer, Third Ed. McGraw-Hill, New York, (1993).

[7]- Jones W.P. and Launder B.E., "The calculation of low-Reynolds number phenomena with a two-equation model of turbulence", *Int. J. Heat Mass Transfer*, **16**, (1973), pp.1119-1130.

[8]- Launder B.E. and Sharma B.I., "Application of the energy dissipation model of turbulence to the calculation of flow near a spinning disc", *Letter in Heat and Mass Transfer*, **1**, (1974), pp.131-138.

[9]- Lam C.K.G. and Bremhorst K., "A modified form of the k-ε model for predicting wall turbulence", *Journal of Fluids Engineering*, **103**, (1981), pp.456-460.

[10]- Chien K-Y., "Predictions of channels and boundary-layer flows with a low-Reynolds-number turbulence model", *AIAA Journal*, **20-1**, (1982), pp.33-38.

[11]- Abe K., Kondoh T. and Nagano Y., "A new turbulence model for predicting fluid flow and heat transfer in separating and reattaching flows", *Int. J. Heat Mass Transfer*, **16**, (1994), pp. 1119-1130.

[12]- Hadef R. and Leduc B., "Etude comparative de modèles à bas nombre de Reynolds dans la prédiction d'un écoulement à point de stagnation", *Int. Comm. Heat Mass Transfer*, **29-5**, (2002).

[13]- Patankar S.V., "Numerical Heat Transfer and Fluid Flow", Mc-Graw Hill, New York (1980).

[14]- Leonard B.P., "A Stable and Accurate Convective Modelling Procedure Based on Quadratic Upstream Interpolation", *Comp. Meth. Appl. Mech. Eng.*, **4**, (1979).

[15]- Spalding D., "A Novel Finite Difference Formulation for Differential Expressions Involving both First and Second Derivatives", *J. Numerical Methods in Eng.*, **4**, (1972).

[16]- Issa R.I., "Solution of the Implicitly Discretised Fluid Flow Equations by Operator-Splitting", Rept FS/82/15, Imperial College of Science & Technology, Fluid Section (1983).

[17]- Zhe J. and Modi V., "Near wall measurements for a turbulent impinging slot jet", *ASME-Journal of Fluid Engineering*, (2001), pp. 112-120.

[18]- Baughn J.W. and Shimizu S., "Heat Transfer Measurements from a Surface With Uniform Heat Flux and an Impinging Jet", *ASME J. Heat Transfer*, **111**, (1989), pp. 1096-1098.

[19]- White F.M., Fluid Mechanics, 2nd Ed. McGraw-Hill, New York, (1986).

[20]- Tennekes H. and Lumley J. L., A first course in turbulence, MIT Press (1972).

[21]- Yap C.R., "Turbulent and momentum transfer in a recirculating and impinging flows, Ph.D. thesis, Faculty of Technology, University of Manchester, U.K. (1987).